Dimensionality Features Extraction Based-on Multi-scale Neighborhood of Multi-samples UAV Point Clouds

Mirko Saponaro(✉)

Polytechnic University of Bari, Via Orabona 4, 70125 Bari, Italy
mirko.saponaro@poliba.it

Abstract. The growth in quantity and quality of collected point clouds has made inevitable to find methods of algorithmic interpretation of these data for any engineering analysis. To date, the most critical steps are still usually performed manually. The fully automated analysis of point clouds acquired from the most arising technologies, such as those generated by photogrammetry obtained from the increasing use of Unmanned Aerial Vehicles (UAVs), has therefore become a topic of great involvement. In order to describe the local geometry at a given point, the spatial distribution of the others 3D points within a local neighborhood was typically taken into account. From the analysis of the covariance matrix, it was thus possible to extract the geometric characteristics useful for identifying any linear, planar or scattering behaviors of the digital reconstruction. Hence, a suitable scalar dimensionality approach had to be planned to identify all the interpretable geometric behaviors of the points at various research scales. Subsequently, one can opt for a single representative scale or a multi-scale approach that serves the purpose of the work. The proposal of this work was to analyze the behavior of the scalar dimensional approach but varying the average Ground Sample Distance (GSD) values of UAV imagery of the same scenario. Encouraging results were obtained expressing how the scenario reproduces the same dimensional behavior irrespective of the acquisition conditions and an empirical finding between the scale parameter r and just the geometric resolution value.

Keywords: Covariance features · Neighborhood scale · Point-based · UAV

1 Introduction

The development of techniques and technologies to collect huge point clouds has made unavoidable to find methodologies oriented to an automated interpretation of these data for any engineering application. As pointed out by Weidner et al. [1], this presents an interesting challenge as today the most critical managing steps are still usually performed manually. Manual analysis of these enormous masses of points is clearly time-consuming and laborious and could never guarantee explicit and exclusive information, thus highlighting the need for efficiently techniques able to identify objective features [2]. Blomley et al. [3] stated that being able to extract reliable geometric features from these point

© Springer Nature Switzerland AG 2021
O. Gervasi et al. (Eds.): ICCSA 2021, LNCS 12955, pp. 47–62, 2021.
https://doi.org/10.1007/978-3-030-87007-2_4

clouds is crucial to exploit the full potential of these data, e.g., for structural analysis or object detection. Indeed, starting from the characteristics of the points distribution such as smoothness, regularity and vertical dispersion, these encourage the distinction among the points of the surface or object type they represent [4]. The fully automated analysis of point clouds acquired from the most established technologies, such as those recorded by laser scanners (i.e., Terrestrial or Airborne LS) [5, 6], or also obtained by photogrammetry, in particular those taken from the increasing use of Unmanned Aerial Vehicles (UAVs), has therefore become a topic of great involvement [7–9].

In order to describe the local 3D geometry at a given point, the spatial distribution of the others points within a reasonable local neighborhood is typically taken into account. Hence, identifying the best neighborhood for each point was a main issue for a large variety of works in literature: data down-sampling, template fitting, feature detection and computation, interpolation, registration, segmentation, filtering, or modelling purposes [10–13]. Precisely, an optimal neighborhood may be defined as the largest set of spatially close points that belong to the same object, then able to express some 1D, 2D or 3D features [8, 12]. For example, Weinmann et al. [14] considered the optimal neighborhood of each individual 3D point focusing on the extraction of relevant, but no redundant, features able to increase their distinctiveness. But dealing with the complexity of 3D scenes, caused on the one hand by irregular sampling and on the other hand by the heterogeneity of the objects, involves a considerable computational capacity and detects a variety of available geometric features, often also marginal or poorly weighted. Moreover, the parameterization of the neighborhood is still typically selected with respect to the a priori empirical or heuristic knowledge of the study environment. Several works therefore focused their attention on the improvement of automated interpretation methodologies capable of targeting the learning of certain useful features [14].

Building on established image-based techniques, the idea of analyzing invariant moments has been found to be valuable for observing the geometric properties of point clouds. Indeed, from the analysis of the covariance matrix or the structure tensor calculated within the local neighborhood, one proceeds to the extraction of their geometric characteristics [3]. The obtained eigenvalues were understood as neighborhood features providing additional information useful to discriminate planes, edges, corners, lines and volumes. Trivially, these features describe thus the local spatial distribution of 3D points [6]. In addition, the use of such features ensures their feasibility for heterogeneous and unstructured data and at the same time no a-priori knowledge of the scene was required [12].

The local neighborhood for each point can be defined by a spherical or cylindrical neighborhood with a fixed radius r [15]. Alternatively, it could be identified by setting a fixed number $k \in \mathbb{N}$ of neighbors closest to the point of interest. Regardless of the definition mode, both are based on a scaling parameter that is either a radius or k, which is commonly selected to be identical for all points in the cloud but, ideally, it would be optimal to obtain a variable scaling parameter dependent on the local 3D structure as well as the local point density. Calculating these features at multiple scales results in higher accuracy than for only one scale because objects may have differing properties at different scales of analysis [3]. However, multiscale approaches result in larger feature spaces where it will be necessary to use feature selection schemes appropriate for the

scope of work and at the same time reduce the computational load. Deriving features at a single scale, on the other hand, means that one scale must be considered to describe some features better than others [7]. Therefore, a suitable scalar dimensionality approach can be used to define a targeted geometric behavior of the points. Understandably, the dimensionality of an object also depends on the spatial scale at which it is examined. An object that appears planar up close (at a smaller spatial scale) may be three-dimensional at a larger spatial scale. For example, in Kim et al. [4] at varying spatial scales, considering a histogrammetric distribution of features, the selection of the most useful features was done by observing in which attributes the mean distance between the averages exceeds the mean standard deviation [4]. The creation of a representative inventory is also a function of the size of the smallest event that can be detected. In particular, Williams et al. [16] suggested that the minimum detectable movement, or Level of Detection (LoD), is a key parameter firstly in delineating model dimensionality and subsequently in calculating erosion or rockfall volumes. This involves masking regions of change that exceed a strict threshold at the LoD.

Lastly, in the geometric analysis of point clouds, each individual observation can only be interpreted on the basis of its relations to other elements and its probability of belonging to a certain class of objects [12]. Each class of objects actually shows a characteristic coherence at different spatial scales, so it is crucial to establish invariable features that can represent structural information that is not observable at other scales. Consequently, a suitable scale may depend on the type of the chosen feature. Blomley et al. [3] therefore deduced that when pursuing a covariance approach, the same homogeneous environment at a smaller scale can define more distinctive features, while the distribution of shapes may be significant at a larger scale.

The proposal of this work was to analyze the behavior of the scalar dimensional approach when varying the geometric resolution of point cloud acquisition from UAVs of the same scenario. Given the above considerations, it was key to verify if the deducible spatial characteristics (1D, 2D and 3D) of the same scenario can be considered comparable when varying the acquisition strategy, considering the other conditions fixed.

In Sect. 2, the properties of the covariance matrix and the potential of the geo-metric characteristics that can be deduced as the neighborhood parameter varies were explained. Given the conceptualization of the approach, the same section then described the operations performed on the point clouds. Finally, the results were extensively discussed in the following Sect. 3, indicating the learned remarks in the Conclusion.

2 Methods

2.1 Focus on the Surveyed Area and Field Activities

A portion of the waterfront of about 400 m located on the southern coast of Bari (Apulia Region, Italy) was selected as the investigation site [17]. The area (Fig. 1) has been explored in previous studies because of the complexity of the hydrogeological phenomena to which it is subject, causing advanced instability [18]. An exhaustive description of the latter is presented in Capolupo et al. [19].

A monthly flight campaign was planned between 2018 and 2019, excluding the summer period due to the zonal limits imposed by national regulations. In this research

work, two missions performed on 15 and 16 March 2019 were considered, characterized by two different flight altitudes of 70 m and 100 m Above Ground Level (AGL).



Fig. 1. Study area investigated for the tests in this work (Reference System: RDN2008/UTM zone 33N (NE) (EPSG:6708)). The yellow crosses, with red interiors, represent the distribution of targets measured using GNSS technologies (Color figure online).

The flights were performed with a DJI Inspire 1 v.2 prosumer, equipped with a DJI Zenmuse X3 (focal length 3.61 mm, pixel size 1.56 m, 12.4 MP) on a 3-axis gimbal. The flight plan included for both missions a cruising speed (4.0 m/s) and a front and side overlap of 85% and 75%. The camera was oriented nadirally and the acquisition set in stop-go mode in order to reduce the collection of blurred images due to the settling movements of the vehicle. The position of the UAV was recorded by a low-cost GNSS/INS positioning receiver and saved in the metadata of each image.

Framing the same area but at two different elevations resulted in two Ground Sample Distance (GSD) values of 0.03 m/pix and 0.043 m/pix, respectively. A total of 77 images were collected at 100 m AGL, while 89 images were collected for the flight at 70 m AGL.

The acquisitions described were accompanied by a Global Navigation Satellite System (GNSS) survey campaign of 30 permanent natural targets of appropriate size and color with respect to the characteristics of the images collected (Fig. 1). The measurements were carried out using Leica Viva CS10/GS10 GNSS technology in network Real-Time Kinematic (nRTK) mode based on the Leica SmartNet Italpos network with a final 3D accuracy of 0.02 m. The reference system was RDN2008/UTM zone 33N (NE) (EPSG: 6708).

2.2 Data Processing Planning

The photogrammetric processing of the acquired data was articulated in Agisoft Metashape (v.1.5.2) using an ordinary Intel(R) Core (TM) i7-3970X CPU 3.50GHz hardware, with 16GB of RAM and an NVIDIA GeForce GTX 650 graphics card. The

parameterization used in the processes is summarized in Table 1. The entire workflow adopts the technical findings validated in the extensive literature on currently accepted methodologies for consistent photogrammetric modelling [20].

Table 1. Summary sheet of the parameterization used in Agisoft Metashape processing.

AGISOFT METASHAPE PARAMETRIZATION	
REFERENCE SETTINGS	
Coordinate system	RDN2008/UTM zone 33N (NE) (EPSG:6708)
Initial Principal Point Position (xp, yp)	(0, 0)
Camera positioning accuracy	3 m
Camera accuracy, attitude	10 deg
Marker accuracy (object space)	0.02 m
Marker accuracy (image space)	0.5 pixel
GPS/INS offset vector value	$\Delta x = 0.005 \pm 0.005m$ $\Delta y = 0.100 \pm 0.01m$ $\Delta z = 0.250 \pm 0.01m$
PROCESSES PLANNED	
Estimate image quality	100 m [max, min]: 0.919395, 0.808475 70 [max, min]: 0.907735, 0.843747
Set brightness	100 m [Brightness, Contrast]: 80, 140 (%) 70 m [Brightness, Contrast]: 80, 140 (%)
Alignment cameras	Accuracy: High Generic Preselection: Yes Reference Preselection: Yes Key Point Limit: 0 Tie Point Limit: 0 Adaptive Camera Model Fitting: No
Gradual Selection	Reconstruction Uncertainty: 10 Projection Accuracy: 3 Reprojection Error: 0.4
Optimize cameras	K3, K4, P3, P4: No
Build dense cloud	Quality: High Depth Filtering: Aggressive

Given the optimal results achieved in Capolupo et al. [19], the 30 targets in the two datasets were marked, and 14 Ground Control Points (GCPs) were chosen for model georeferencing. The remaining part of the markers were then considered as Check Points (CPs) of the models.

2.3 Neighborhood Recovery and Features Extraction

Most current approaches to finding features of 3D geometries are based on features derived from the local covariance matrix representing the invariant second-order moments within the point positions [3]. In particular, it is possible to extract from the covariance matrix three eigenvalues ($\lambda_1 > \lambda_2 > \lambda_3$) through the statistical Principal Component Analysis (PCA). These represent the local 3D structure and each one measure the variation of the local point set along the direction of the corresponding eigenvector. Briefly, the PCA defines the principal directions in three orthogonal vectors and the respective point distribution variation magnitude around the center of the defined neighborhood, named centroid, in the eigenvalues [12]. The proportions of variance explained by each eigenvalue are defined as:

$$PCA(1) = \lambda_1/(\lambda_1 + \lambda_2 + \lambda_3) \tag{1}$$

$$PCA(2) = \lambda_2/(\lambda_1 + \lambda_2 + \lambda_3) \tag{2}$$

$$PCA(3) = \lambda_3/(\lambda_1 + \lambda_2 + \lambda_3) \tag{3}$$

As explained in Fig. 3 in Brodu et al. [11], the triangular domain of all possible proportions represents the dimensionality cases of the model as the weight of each eigenvalue varies. Given the constraint:

$$PCA(1) + PCA(2) + PCA(3) = 1 \tag{4}$$

when only a single eigenvalue λ_1 accounts for the total variance in the neighborhood sphere the points are oriented along one dimension. Alternatively, when two eigenvalues were necessary to account for the variance but the third one does not contribute the cloud is locally mostly planar. Conversely, a fully 3D cloud is one where all three eigenvalues have the same magnitude. The proportions of eigenvalues thus define a measure of how much 1D, 2D or 3D the cloud appears locally at a given scale.

Moreover, the combination of these eigenvalues generates some shape descriptors, designed to point out a prevalent linear, planar or scatter behavior of the neighborhood, otherwise other measures such as omnivariance, anisotropy and eigenentropy. These local 3D shape features are called eigen-features.

The feature of linearity is used to investigate whether a set of points can be modeled by a 3D line [21]:

$$L = (\lambda_1 - \lambda_2)/\lambda_1 \tag{5}$$

The planarity feature is used to describe the smoothness of a surface:

$$P = (\lambda_2 - \lambda_3)/\lambda_1 \tag{6}$$

The feature of sphericity investigates the scattering of a neighborhood:

$$S = \lambda_3/\lambda_1 \tag{7}$$

Following, the feature of omnivariance describes how a neighborhood of points spread inhomogeneously across a 3D volume:

$$O = (\lambda_1 * \lambda_2 * \lambda_3)^{\frac{1}{3}} \tag{8}$$

Anisotropy is a measure which is higher if the eigenvectors differ a lot. These measures have the potential to discriminate between orientated and non-orientated objects, as oriented objects have a higher anisotropy [22]:

$$A = (\lambda_1 - \lambda_3)/\lambda_1 \tag{9}$$

Lastly, the feature of eigenentropy provides a measure of the order or disorder of 3D points within the covariance ellipsoid [14]:

$$E_\lambda = -(\lambda_1 * \ln\lambda_1 - \lambda_2 * \ln\lambda_2 + \lambda_3 * \ln\lambda_3) \tag{10}$$

Eigenentropy values tending towards 1 identify disturbances within the ellipsoid, thus highlighting the presence of points with 3D behavior. Vice versa, values up to 0 detect an increasing order, passing from planar to linear dimensionality.

One of the approaches proposed by Weinmann et al. [14] for the identification of a suitable scaling parameter for the dimensional analysis of models analyses the change in curvature by means of the PCA (3) value. The curvature using PCA (3) is then calculated as seen in Eq. (3) from the ratio of the minimum eigenvalue to the sum of the eigenvalues. This ratio approximates the change in curvature in the vicinity of a point. Given the fact that the accreted jumps indicate strong deviations in the normal directions, a suitable scaling parameter value would identify concordant values of PCA (3) and thus be able to describe various consistent levels of curvature.

The most common approach to defining a local neighborhood depends on a user-defined radial distance r or a fixed value k of neighborhood points. In this research work, the radius approach was adopted. The radius defines a spherical or cylindrical volume within which the neighborhood of points is incorporated. The radius must be large enough to incorporate enough points to calculate meaningful statistics, but not so large as to lose spatial detail [4]. The expressible geometric features will therefore be influenced by the search radius, which determines the size of the neighborhood over which these features will be calculated. In addition, autocorrelation and other features might only be observed at some scales less than at others [3]. In many works of literature therefore, authors propose different approaches in order to identify the most suitable research parameter r for different purposes, already mentioned in the Sect. 1. It is the nature of second-order moments that the distance of an element from the mean contributes quadratically and thus elements in the vicinity are less important than those further away [3]. Since principal component analysis is an orthogonal transformation and therefore unitary, the resulting eigenvalues are sensitive to the original scale. It remains to be shown whether this optimal neighborhood dimension for covariance characteristics corresponds to the characteristic scale of any structure. The scale-based dimensional approach finds, for each 3D point, the optimal search radius by computing the neighborhood at different and increasing radii (between a minimum and a maximum value) and selecting the one that minimizes a measure of unpredictability of the set of points.

The dense point clouds obtained in the previous step were then imported in the open-source software CloudCompare. Given the GSD values (m/pix) described in Sect. 2.1, the following features were computed using the Computes Geometries tool:

– 1st, 2nd and 3rd Eigenvalues (λ_1, λ_2, λ_3)
– PCA (1), PCA (2) and PCA (3)
– Anisotropy and Omnivariance
– Linearity, Planarity and Sphericity
– Eigenentropy.

These were computed for ten values of the scale-parameter r of sphere, varying the latter from a minimum equal to the value of the GSD and from time to time multiplying it up to 10. Table 2 summarizes the values of r for the two cases under study. The behaviors of these characteristics were analyzed and finally the most significant dimensionality behaviors were identified by observing the Eigenentropy trends.

Table 2. Summary of the used scale parameters r.

r	[70 m]	[100 m]
*GSD * 1*	0.030 m	0.043 m
*GSD * 2*	0.060 m	0.086 m
*GSD * 3*	0.090 m	0.129 m
*GSD * 4*	0.120 m	0.172 m
*GSD * 5*	0.150 m	0.215 m
*GSD * 6*	0.180 m	0.258 m
*GSD * 7*	0.210 m	0.301 m
*GSD * 8*	0.240 m	0.344 m
*GSD * 9*	0.270 m	0.387 m
*GSD * 10*	0.300 m	0.43 m

3 Results and Discussion

3.1 Eigenvalues Behaviors

The recorded trends of the eigenvalues as the scale parameter r changes in the two dense point clouds obtained from images acquired at 70 m and 100 m AGL were analyzed below.

Figure 2 shows how, in general, the behaviors recorded for the two cases were completely comparable even if the scale parameter r varies. In fact, the values of the eigenvalues undergone a reproportioning, approximately double, passing from the [70 m] to the [100 m] case. This suggests that the magnitude of the eigenvalues was proportional

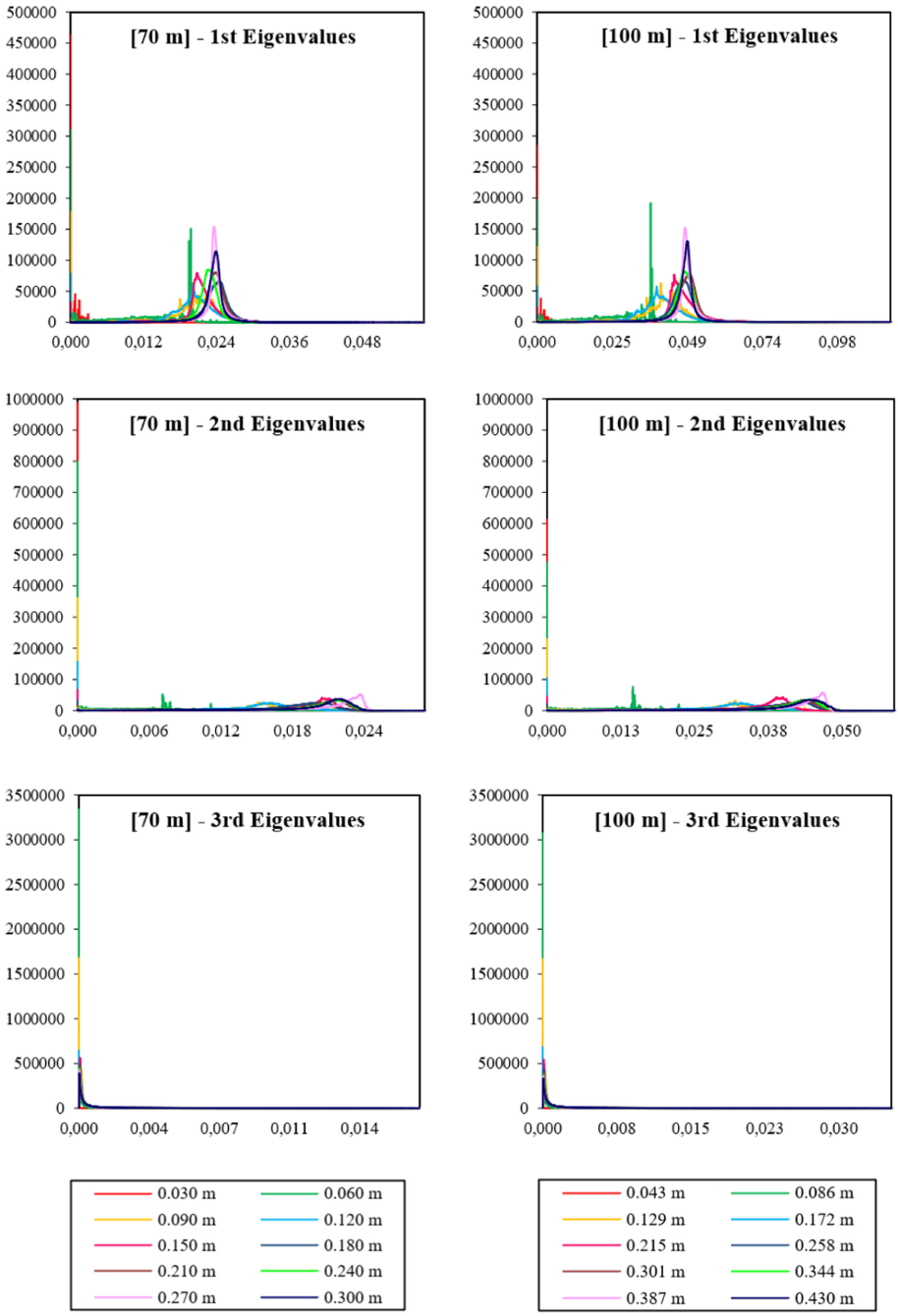

Fig. 2. Histograms of the three eigenvalues as the scale parameter r changes. The abscissae show the values of the eigenvalues, the ordinates the number of points in each class. Below is the legend with the colour scale for each scale parameter r.

to the UAV acquisition altitude and that, as the GSD value increases, the Principal Component Analysis (PCA) approach reiterates the dimensional traces already inferred at the lower altitude.

Analyzing the behavior as r varies in the 1st Eigenvalues, decreasing peaks were observed for r values starting from 0.030 m and 0.060 m. The remaining part of the cases are positioned on magnitudes equal to about 0.024 for the [70 m] case and 0.049 for [100 m]. Amongst these, the r-scale parameters of 0.387 m and 0.430 m show more pronounced peaks around those values. The first eigenvalue can be considered fundamental to discriminate those scaling parameters that are efficient in the calculation of the dimensionality of the point clouds. As in fact already discussed by Brodu et al. [11], null values of the 1st eigenvalue would void the triangular domain hypothesis while a very low magnitude would detect a weak orientation along the respective eigenvector, making the measurement unreliable. It was therefore clear that for scale parameters below 0.090 m [70 m] and 0.129 m [100 m], the PCA approach fails to accurately describe the geometric behavior of the clouds.

On the other hand, analyzing the 2nd Eigenvalues, for r values lower than 0.172 m the points fallen mainly around 0, while for the remaining scale parameters distributions between 0.018–0.024 in the case of [70 m] and 0.038–0.050 in the case of [100 m] were observed. In the 3rd Eigenvalues cases, it is evident that they assumed values around 0, thus highlighting already in this first step a non 3D behavior of both photogrammetric reconstructions.

3.2 PCA Features

The trends recorded in the PCA (1,2,3) variance proportions as the scale parameter r changes in the two dense point clouds obtained from images acquired at 70 m and 100 m AGL were analyzed below.

The histograms presented in Fig. 3 confirmed what has already been stated in the previous paragraph, i.e., given comparable behavior, a slight increase in the magnitude of each variance proportion is observed in the [100 m] case.

In the first two histograms increasing peaks in the PCA (1) value for scale parameters r lower than 0.120 m [70 m] and 0.129 m [100 m] were observed, passing from a predominantly planar behavior (greater than 0.33, threshold of three-dimensionality) to a linear one when it assumed a value equal to 1. In the remaining part of the cases this settles at around a PCA (1) value of 0.500, identifying predominantly planar behavior. The considerations were confirmed by observing the PCA (2) histograms, in which the same scale parameters mentioned above assume a value of 0, while in the remaining part of the cases it tends to 0.500. Finally, for the PCA (3) cases, as already stated in the previous paragraph, this assumed values predominantly equal to 0, ascertaining that the PCA approach did not succeed in identifying three-dimensional behavior.

3.3 Geometric Features

Figure 4 analyzed the trends of the Geometric Features Anisotropy and Omnivariance as the scale parameter r changes in the two dense point clouds obtained from images acquired at 70 m and 100 m AGL.

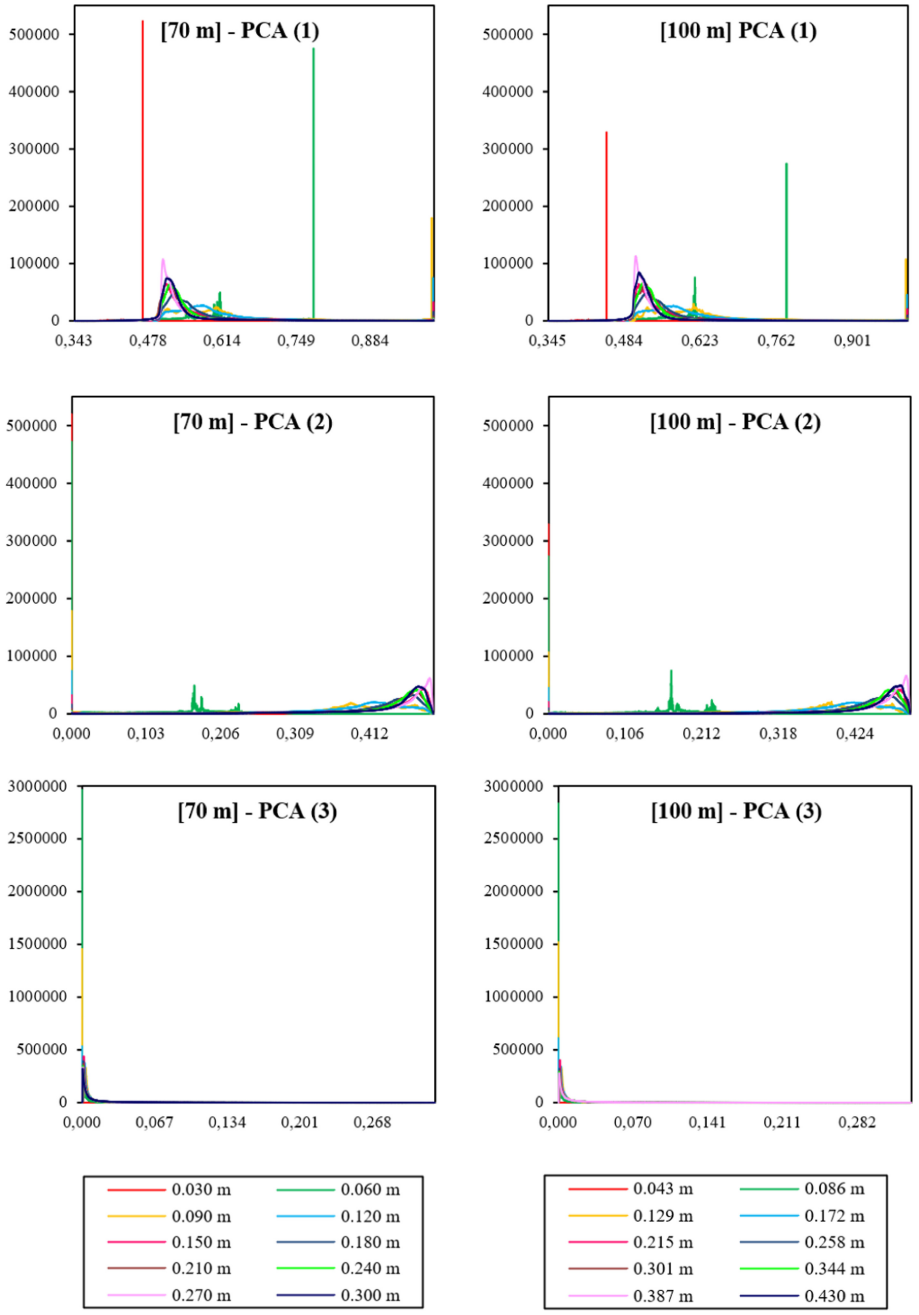

Fig. 3. Histograms of the three eigenvalues as the scale parameter r changes. The abscissae show the values of the eigenvalues, the ordinates the number of points in each class.

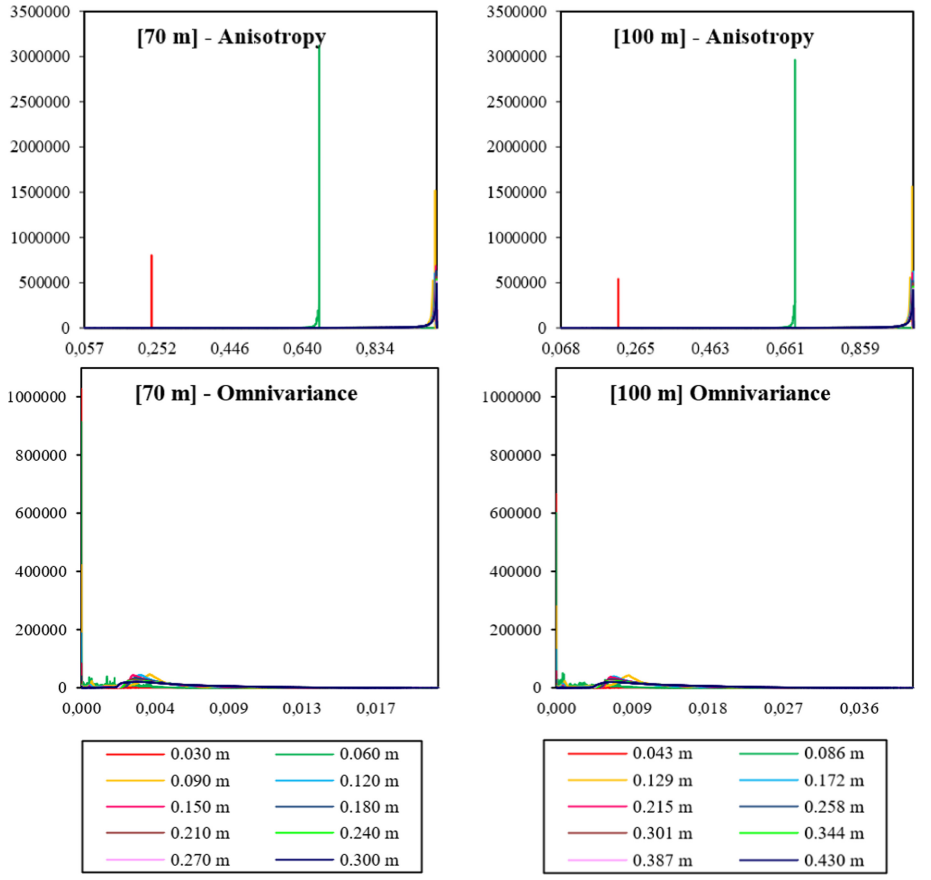

Fig. 4. Histograms of the Anisotropy and Omnivariance as the scale parameter r changes. The abscissae show the values of the eigen-features, the ordinates the number of points in each class.

Higher values of anisotropy identify the presence of eigenvalues (λ_1, λ_3) on eigenvectors that differ greatly. This, however, leads to discriminate oriented objects (high anisotropy) from non-oriented objects, and therefore to discriminate possible dimensionality: in particular, a value of 0 defines an isotropy, i.e. a three-dimensional behaviour, vice versa for values equal to 1 the behaviour will be 1D. The obtained histograms confirmed what has already been discussed.

The values of Ominivariance tending to 0.33 identify three-dimensional behaviour, while at 0 a linear attitude. It was evident how these were concentrated for values equal to 0.004 and 0.009 for the cases [70 m] and [100 m], respectively: therefore, a planar behaviour.

Figure 5 analyzed the trends of the geometric features Linearity and Planarity as the scale parameter r varies in the two dense point clouds obtained from images acquired at 70 m and 100 m AGL. It has been chosen not to propose the histograms concerning

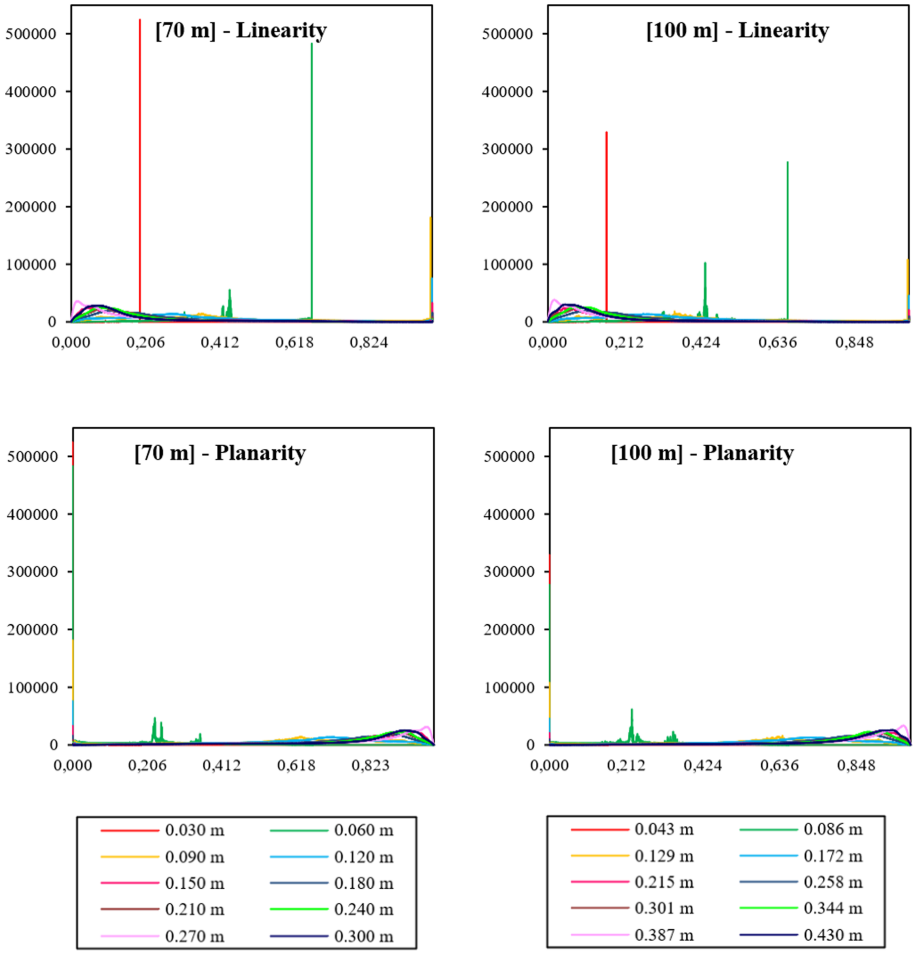

Fig. 5. Histograms of linearity and planarity as the scale parameter r changes. The abscissae show the values of the eigen-features, the ordinates the number of points in each class.

Sphericity as they were not significant by proposing values equal to 0, not demonstrating anything else than what has already been discussed.

The histograms complete the discussion examined so far. Since there were no significant three-dimensional behaviors, the two represented geometric characteristics were almost complementary.

3.4 Eigenentropy Analysis

The entropy function provides for each reconstructed 3D point a measure of the probability of belonging to a part of the scene with a specific geometric behavior. High entropy values, i.e., tending to 1, indicate a disordered geometric behavior of the neighboring point

and, most likely, the non-planar nature of these points. On the contrary, values lower than about 0.7 identify first a planar behavior, then a linear one until they cancel out.

Since the discussed eigenvalues (λ_1, λ_2, λ_3) were values obtained from the minimization for each point of the Eigenentropy value of the ellipsoid, the histograms in Fig. 6 represented the distribution of the significant features in the investigated area. Very spanned distributions of the latter identified a non-univocal behavior of all points and therefore the chosen scaling parameter r was not sufficiently uniform and descriptive of the whole scenario. Peak distributions, on the other hand, showed that the scaling parameter r can be considered optimal, i.e., it can best explain the prevailing dimensionalities of the scenario. Therefore, from a general survey, histograms with scale parameter r obtained by multiplying the GSD value by 9 and 10 were the most efficient. Thus, r-scale parameters one order higher than the GSD value were able to qualitatively and quantitatively better identify the dimensionality of the survey carried out, regardless of the used acquisition strategy.

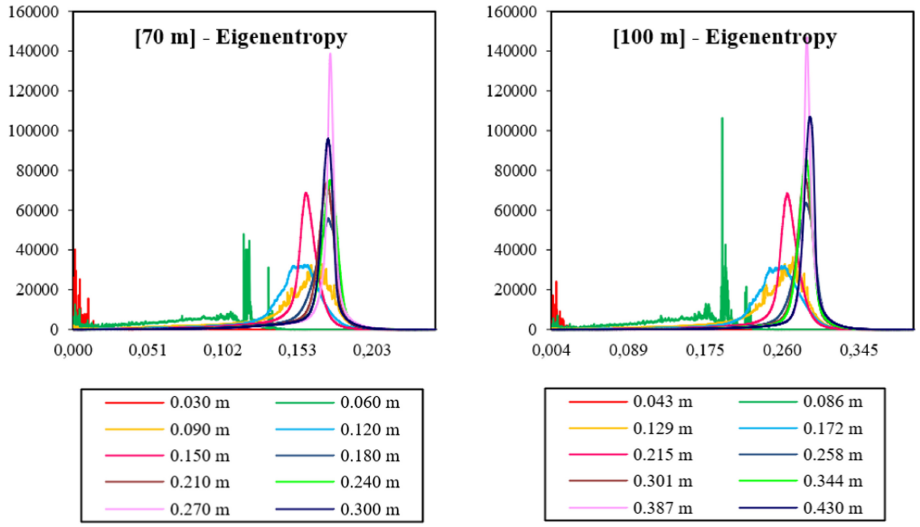

Fig. 6. Histograms of eigenentropy as the scale parameter r changes. The abscissae show the values of the eigen-feature, the ordinates the number of points in each class.

4 Conclusion

The increase of high-density and accurate UAV-based point clouds has made challenging to structure fully automated methods for feature-interpretation of these data for various applications, i.e., segmentation, classification, filtering and dimensional feature learning for cloud-to-cloud analysis. In order to describe the local geometry at a given point, the spatial distribution of the others 3D points within a local neighborhood is typically taken into account. From the covariance matrix it is possible to extract the geometric characteristics useful for identifying any linear, planar or scattering behaviors of the point clouds.

The proposal of this work was to analyze the behavior of the scalar dimensional approach but varying the average GSD values of two UAV dataset of the same scenario. The results achieved demonstrate how this field of application can advance new point-based learning methodologies useful for the extraction of valid morphological information. In general, the behaviors recorded for the two different flight height cases were completely comparable even if the scale parameter r varies. In fact, the values of geometric features undergone a reproportioning passing from the [70 m] to the [100 m] case. This suggests that the magnitude of the eigenvalues was proportional to the UAV acquisition altitude and that, as the GSD value increases, the PCA approach reiterates the dimensional traces already inferred at the lower altitude. At last, r-scale parameters one order higher than the GSD value were able to qualitatively and quantitatively better identify the dimensionality of the survey carried out, regardless of the acquisition strategy used. Considering the findings outlined above, further processing and interpretation can be structured to exploit the dimensionality information provided.

References

1. Weidner, L., Walton, G., Krajnovich, A.: Classifying rock slope materials in photogrammetric point clouds using robust color and geometric features (2021)
2. Jafari, B., Khaloo, A., Lattanzi, D.: Deformation tracking in 3D point clouds via statistical sampling of direct cloud-to-cloud distances. J. Nondestr. Eval. **36**(4), 1 (2017). https://doi.org/10.1007/s10921-017-0444-2
3. Blomley, R., Weinmann, M., Leitloff, J., Jutzi, B.: Shape distribution features for point cloud analysis - a geometric histogram approach on multiple scales. ISPRS Ann. Photogramm. Remote Sens. Spatial Inf. Sci. **II-3**, 9–16 (2014)
4. Kim, A., Olsen, R., Kruse, F.: Methods for LiDAR point cloud classification using local neighborhood statistics. SPIE (2013)
5. Mallet, C., Bretar, F., Roux, M., Soergel, U., Heipke, C.: Relevance assessment of full-waveform lidar data for urban area classification. ISPRS J. Photogramm. Remote. Sens. **66**, S71–S84 (2011)
6. Chehata, N., Guo, L., Mallet, C.: Airborne lidar feature selection for urban classification using random forests. In: Laserscanning (2009)
7. Weinmann, M., Schmidt, A., Mallet, C., Hinz, S., Rottensteiner, F., Jutzi, B.: Contextual classification of point cloud data by exploiting individual 3D neigbourhoods. ISPRS Ann. Photogramm. Remote Sens. Spatial Inf. Sci. **II-3/W4**, 271–278 (2015)
8. Farella, E.M., Torresani, A., Remondino, F.: Quality features for the integration of terrestrial and UAV images. Int. Arch. Photogramm. Remote Sens. Spatial Inf. Sci. **XLII-2/W9**, 339–346 (2019)
9. Karantanellis, E., et al.: Evaluating the quality of photogrammetric point-clouds in challenging geo-environments – a case study in an Alpine Valley. Int. Arch. Photogramm. Remote Sens. Spatial Inf. Sci. **XLIII-B2–2020**, 1099–1105 (2020)
10. Demantké, J., Mallet, C., David, N., Vallet, B.: Dimensionality based scale selection in 3D lidar point clouds. In: Laserscanning (2011)
11. Brodu, N., Lague, D.: 3D terrestrial lidar data classification of complex natural scenes using a multi-scale dimensionality criterion: applications in geomorphology. ISPRS J. Photogramm. Remote. Sens. **68**, 121–134 (2012)
12. Farella, E.M., Torresani, A., Remondino, F.: Sparse point cloud filtering based on covariance features. Int. Arch. Photogramm. Remote Sens. Spatial Inf. Sci. **XLII-2/W15**, 465–472 (2019)

13. Weidner, L., Walton, G., Kromer, R.: Classification methods for point clouds in rock slope monitoring: a novel machine learning approach and comparative analysis. Eng. Geol. **263**, 105326 (2019)
14. Weinmann, M., Jutzi, B., Mallet, C.: Semantic 3D scene interpretation: a framework combining optimal neighborhood size selection with relevant features. ISPRS Ann. Photogramm. Remote Sens. Spatial Inf. Sci. **II-3**, 181–188 (2014)
15. Thomas, H., Goulette, F., Deschaud, J.-E., Marcotegui, B., LeGall, Y.: Semantic classification of 3D point clouds with multiscale spherical neighborhoods. In: 2018 International Conference on 3D Vision (3DV). IEEE, pp. 390–398 (2018)
16. Williams, J.G., Rosser, N.J., Hardy, R.J., Brain, M.J., Afana, A.A.: Optimising 4-D surface change detection: an approach for capturing rockfall magnitude–frequency. Earth Surf. Dynam. **6**, 101–119 (2018)
17. Saponaro, M., Capolupo, A., Tarantino, E., Fratino, U.: Comparative Analysis of Different UAV-Based Photogrammetric Processes to Improve Product Accuracies. In: Misra, S., et al. (eds.) ICCSA 2019. LNCS, vol. 11622, pp. 225–238. Springer, Cham (2019). https://doi.org/10.1007/978-3-030-24305-0_18
18. Saponaro, M., Tarantino, E., Reina, A., Furfaro, G., Fratino, U.: Assessing the impact of the number of GCPS on the accuracy of photogrammetric mapping from UAV imagery. Baltic Surveying 43 (2019)
19. Capolupo, A., Saponaro, M., Borgogno Mondino, E., Tarantino, E.: Combining interior orientation variables to predict the accuracy of Rpas-Sfm 3D models. Remote Sens. **12**, 2674 (2020)
20. Saponaro, M., Turso, A., Tarantino, E.: Parallel Development of Comparable Photogrammetric Workflows Based on UAV Data Inside SW Platforms. In: Gervasi, O., et al. (eds.) ICCSA 2020. LNCS, vol. 12252, pp. 693–708. Springer, Cham (2020). https://doi.org/10.1007/978-3-030-58811-3_50
21. Waldhauser, C., et al.: Automated classification of airborne laser scanning point clouds. In: Solving Computationally Expensive Engineering Problems. Springer, pp. 269–292 (2014)
22. Elberink, S.O., Maas, H.-G.: The use of anisotropic height texture measures for the segmentation of airborne laser scanner data. Int. Archiv. Photogram. Remote Sens. **33**, 678–684 (2000)